Journal of Hydrology 621 (2023) 129610

Contents lists available at ScienceDirect

Journal of Hydrology

journal homepage: www.elsevier.com/locate/jhydrol

Research papers

Evaluating the influence of boulder arrangement on flow resistance in gravel-bed channels

A. Nicosia [a], F.G. Carollo [a], V. Ferro [a,b,*]

[a] Department of Agricultural, Food and Forest Sciences, University of Palermo, Viale delle Scienze, Building 4, Palermo 90128, Italy
[b] NBFC, National Biodiversity Future Center, Palermo 90133, Italy

ARTICLE INFO

Keywords:
Gravel bed
Dimensional analysis
Flow resistance
Flow velocity profile
Boulder arrangement
Self-similarity

ABSTRACT

Gravel bed flow resistance is affected by the shape and size of the roughness elements and their arrangement on the channel bed surface (spacing between elements, direction with respect to flow streamlines, and protrusion of the elements from the channel bed). Previous studies demonstrated that the flow resistance of open channel flows can be obtained by integrating the power velocity profile. This paper aims to study flow resistance in gravel-bed channels with different concentrations of boulders having staggered arrangements. At first, the equation relating Γ coefficient of the power velocity profile, and the Froude number was calibrated using measurements performed in a flume covered by hemispheric roughness elements for partially submerged and completely submerged hydraulic conditions. The roughness elements were evenly spaced (staggered) and arranged using three different concentrations of 9, 25, and 49%. Moreover, the relationship between Γ, slope, and the Froude number, calibrated using literature measurements performed with the same experimental setup but with a square arrangement, was tested for the measurements obtained with the staggered arrangement. The results showed that i) the Darcy-Weisbach friction factor can be accurately estimated by the proposed flow resistance equation, ii) the differences in flow resistance behavior between the two different investigated arrangements (staggered, square) occur only for the partially submerged hydraulic condition, and iii) for the staggered arrangement, skimming flow is reached for lower element concentrations as compared to the square one.

1. Introduction

The estimate of flow velocity in gravel-bed rivers is a widely studied topic, but some scientific and technical aspects have to be still clarified. For gravel-bed channels, the large-scale roughness condition (Bathurst, 1978; Bray, 1979; Bray, 1982; Lawrence, 1997) is characterized by a mean flow depth h comparable with the bed roughness size. Some Authors (Bathurst et al., 1981; Colosimo et al., 1988; Reid and Hickin, 2008; Mendicino and Colosimo, 2019) suggested that if the hydraulic condition is defined by the ratio between the flow depth and the bed particle diameter d_{84} (diameter for which 84% of the particles are finer), a large-scale occurs for $h/d_{84} \leq 4$. Large and small-scale roughness conditions are characterized by different dissipative mechanisms. Bathurst et al. (1981) stated that the depth/sediment ratio, i.e., the ratio between the hydraulic radius R or h and the particle diameter representing the characteristic roughness height, is associated to different dissipative mechanisms. According to Mendicino and Colosimo (2019), for high values of this ratio (>100), skin friction is due to drag effects related to the shape of individual bed particles and viscous friction on their surfaces, and it is also affected by large scale bed-forms.

When relative submergence is low, i.e., $h/d_{84} \leq 10$ and more specifically h/d_{84} is close to 1, the resistance effects due to form drag and turbulent wakes caused by large roughness elements increase. Further energy losses occur when the flow is locally supercritical and if some elements protrude above the water surface (Ferguson, 2007; Rickenmann and Recking, 2011, Nitsche et al., 2012; Mendicino and Colosimo, 2019).

At present, the flow resistance of uniform open channel flows for small-scale roughness is more investigated than that occurring in a large-scale condition.

In previous studies (Powell, 2014), the open channel flow resistance equation was theoretically obtained for some known cross-section shapes (circular and very wide rectangular) and established boundary conditions, for which the velocity distribution is known. The integration of the flow-velocity profile allowed to obtain a semi-theoretical flow resistance equation (Ferro, 2003a; Ferro, 2003b; Powell, 2014; Ferro

* Corresponding author at: Department of Agricultural, Food and Forest Sciences, University of Palermo, Viale delle Scienze, Building 4, Palermo 90128, Italy.
E-mail address: vito.ferro@unipa.it (V. Ferro).

https://doi.org/10.1016/j.jhydrol.2023.129610
Received 24 September 2022; Received in revised form 3 April 2023; Accepted 27 April 2023
Available online 4 May 2023

and Porto, 2018a; Ferro and Porto, 2018b), which is the main tool required in open channel flow hydraulics.

When the open channel flow is two-dimensional and the occurring roughness condition is "small-scale" (h/d_{50} >20 (Bray, 1987) or h/d_{84} >4 (Bathurst, 1982)), the logarithmic velocity distribution is applied in both the fully turbulent part of the inner region and the outer region (Coleman and Alonso, 1983; Kirkgöz, 1989). Flow velocity profiles measured in a gravel-bed flume (Bathurst, 1988; Ferro and Baiamonte, 1994) demonstrated that the logarithmic velocity distribution can be applied for a bottom distance $y < y_{max}$, where y_{max} is the distance at which the maximum flow velocity is located. For a small-scale roughness condition, a semi-logarithmic flow resistance law is obtained by integrating the logarithmic velocity distribution (Bray, 1987; Smart et al., 2002; Ferguson, 2007; Chen et al., 2020; Singh et al., 2021). For small and large-scale roughness, Ferro and Pecoraro (2000) deduced a power velocity profile by using the incomplete self-similarity theory. Moreover, measured distributions having the measured maximum velocity located at the free surface were used to fit the power velocity profile.

For a large-scale roughness condition ($h/d_{84} \leq 4$), previous velocity measurements (Marchand et al., 1984; Bathurst, 1988) demonstrated that the velocity profile is S-shaped, with near-surface velocity higher than near-bed ones, and the logarithmic or power distribution can be assumed only for bottom distance y greater than the roughness size.

Ferro (1999) performed flume experiments for transition and large-scale roughness conditions using boulders with a coverage degree ranging from 0 to 83%, arranged on a quarry rubble bed and pointed out that a skimming flow regime (Morris, 1959) occurs for high boulder concentrations (>50%). In this flow regime, the roughness elements are so close that between them an eddy is confined, and the flow motion occurs on a surface placed at the top level of the elements.

The estimate of the flow velocity from the knowledge of the cross-section shape and sizes, depth, and the bed slope continues to be one of the most relevant hydraulic topics (Rouse and Ince, 1963; Bray 1982). The Chezy, the Manning, and the Darcy-Weisbach uniform flow resistance formulas are currently applied (Rouse and Ince, 1963; Bray, 1982; Powell, 2014):

$$V = C\sqrt{Rs} = \frac{s^{1/2}R^{2/3}}{n} = \sqrt{\frac{8gRs}{f}} = u_*\sqrt{\frac{8}{f}} \tag{1}$$

where V is the cross-section average velocity, C is the Chezy coefficient ($m^{1/2}$ s^{-1}), n is the Manning coefficient ($m^{-1/3}$ s), f is the Darcy-Weisbach friction factor, s is the channel slope, g is the gravitational acceleration and $u_* = \sqrt{g\,R\,s}$ is the shear velocity, where R is the hydraulic radius.

For a uniform turbulent open channel flow, the vertical velocity profile distribution can be represented by the following equation (Barenblatt, 1979; Barenblatt, 1987; Barenblatt, 1993; Barenblatt and Monin, 1979; Barenblatt and Prostokishin, 1993):

$$\frac{v}{u_*} = \Gamma\left(\frac{u_* y}{\nu_k}\right)^{\delta} \tag{2}$$

in which v is the local velocity, y is the distance from the bottom, ν_k is the kinematic viscosity, Γ is a function estimated by experimental velocity measurements, and δ is an exponent calculated by the following relationship (Castaing et al., 1990; Barenblatt, 1991):

$$\delta = \frac{1.5}{\ln Re} \tag{3}$$

in which $Re = V\,h/\nu_k$ is the flow Reynolds number.

Integrating Eq. (2), the following expression of the Darcy-Weisbach friction factor f (Barenblatt, 1993; Ferro, 2017) is obtained:

$$f = 8\left[\frac{2^{1-\delta}\Gamma Re^{\delta}}{(\delta+1)(\delta+2)}\right]^{-2/(1+\delta)} \tag{4}$$

Hypothesizing that $y = \alpha\,h$ (i.e., the distance from the bottom where the local velocity is equal to the cross-section average velocity V), Eq. (2) gives the following estimate Γ_v of the function Γ (Ferro, 2017):

$$\Gamma_v = \frac{V}{u_*\left(\frac{u_*\alpha h}{\nu_k}\right)^{\delta}} \tag{5}$$

where α <1 is a coefficient which states two conditions: (i) the average flow velocity V occurs below the water surface and (ii) a single velocity profile is used to express the velocity distribution for the whole cross-section.

Ferro (2017) theoretically deduced the following equation for calculating α:

$$\alpha = \left[\frac{2^{1-\delta}}{(\delta+1)(\delta+2)}\right]^{1/\delta} \tag{6}$$

Eqs. (4) and (5) were tested by Ferro (2017), who used field measurements of flow velocity, water depth, river width and bed slope performed in some Canadian mountain streams (Reid and Hickin, 2008). According to the theoretical analysis developed by Ferro (2018), the estimate Γ_v of the Γ function can be expressed by the following power equation:

$$\Gamma_v = a\frac{F^b}{s^c} \tag{7}$$

where $F = V/\sqrt{g\,h}$is the flow Froude number and a, b, and c are coefficients to be estimated by experimental measurements.

For a constant s value, Eq. (7) becomes:

$$\Gamma_v = a_o F^b \tag{8}$$

in which the coefficient a_o and b have to be estimated by measurements.

The applicability of Eq. (7) was tested by Ferro and Porto (2018a) and Ferro (2018) using flume measurements (Ferro and Giordano, 1991; Ferro and Baiamonte, 1994; Baiamonte et al., 1995; Ferro and Pecoraro, 2000) and gravel-bed river data (Bathurst, 1978; Bathurst, 1985; Bray, 1979; Ferro and Porto, 2018a; Griffiths, 1981; Kellerhals, 1967; Thompson and Campbell, 1979).

Ferro (2018) also demonstrated that Eq. (7), with a, b, and c coefficients estimated by flume data, can be applied to measurements carried out in gravel-bed rivers (Reid and Hickin, 2008) using a scale factor equal to 0.7611 (Ferro and Porto, 2019).

Carollo and Ferro (2021), using measurements conducted in a flume covered by hemispheric elements for two different hydraulic conditions (partially submerged and completely submerged), positively tested Eq. (7). For their experiments, the elements were placed with a square arrangement and a concentration C_h varying from 4 to 64%. For the two investigated hydraulic conditions, the same exponents b (1.1295) and c (0.595) of Eq. (7), but a different scale factor a (0.3261 for partially submerged and 0.3013 for completely submerged) were obtained. These Authors also found that, for the partially inundated condition (h/d <1) and concentration C_h <25%, the scale factor increased with C_h, whereas, for 25% $\leq C_h \leq$ 64%, a decreased with C_h. For $h/d \geq 1$, the scale factor increased with C_h, while it became almost constant for $C_h \geq$ 49%.

For large-scale roughness conditions, the shape and size of the roughness elements and their arrangement (spacing between elements, direction with respect to flow streamlines, and protrusion of the elements from the channel bed) affect flow resistance (Bathurst, 1978; Bathurst et al., 1981; Lawrence, 1997; Nicosia et al., 2023; O'Loughlin and Macdonald, 1964; Pyle and Novak, 1981; Thompson and Campbell, 1979).

O'Loughlin and Macdonald (1964) carried out flume experiments to evaluate overall flow resistance for two roughness elements having a different shape (cube and sand) characterized by different concentrations. This analysis showed that for the cube roughness with high

concentration values (0.7), the regularity of the investigated surface allows the development of skimming flow.

For a wide range of flow conditions in terms of submergence ratio h/d, Lawrence (1997) examined available literature data to assess the overland flow resistance. The results confirmed a non-monotonic dependence between friction factor and h/d and supported the existence of three flow regimes based on the submergence ratio. For the partially and marginally submerged regimes, Lawrence (1997) found that the roughness element concentration and the surface slope affect the friction factor, while the effect of the Reynolds number should be significant only for well-submerged flows at low to moderate Reynolds numbers. As these Re values are quite rare in field conditions, the h/d ratio rather than Re should be considered as the main dimensionless group affecting the hydraulics of overland flow on rough surfaces.

Lawrence (2000) carried out experiments on overland flow in a flume with the bed covered by hemispheric elements. Flow resistance rapidly decreases when the roughness elements are well submerged and further decreases for increasing water depth values. Moreover, the results showed that flow resistance increases for increasing element concentrations.

When boulder concentration is low, the roughness elements are so distant that dissipation of the wake generated by each element occurs before approaching the next element along the flow direction (semi-smooth isolated roughness turbulent flow) (Morris, 1959; Yen, 2002; Zexing et al., 2020). For increasing values of boulder concentration, the elements are so close that the wake cannot dissipate before the approach to the next one (wake interference flow). Consequently, the effect of interference between roughness elements on flow resistance increases, while that of the arrangement of the boulders (for example, square or staggered) decreases.

In previous papers, the effect of boulder concentration on flow resistance was examined by using gravel boulders arranged on a quarry rubble bed (Ferro and Giordano, 1991; Ferro, 1999; Ferro, 2003b), while in this study smooth hemispherical elements are used. This choice allowed to avoid the effect of the boulder shape variability and surface roughness of the coarse size elements on the friction factor. Furthermore, to the best of our knowledge, there is a lack of investigations on the effects of the boulder arrangement on flow resistance for low values of C_h in which this effect is dominant.

This paper aims to isolate these arrangement effects in gravel-bed channels characterized by different boulder concentrations using experiments that were performed with the same experimental conditions by Carollo and Ferro (2021) but with a staggered arrangement of the elements.

In particular, this paper aims to: (i) calibrate Eq. (7) using laboratory flume measurements carried out for different hydraulic conditions (large-scale, transition, and small-scale roughness), and hemispheric elements having a staggered arrangement and a concentration ranging from 9 to 49%; (ii) evaluate the effect of the elements' arrangement on Darcy-Weisbach friction factor; and (iii) compare the flow resistance behavior of square and staggered arrangements by measurements carried out in the same experimental conditions.

2. Materials and methods

The measurements were performed in a glass-bed and walls laboratory flume (Fig. 1) (length 14.4 m, width 0.6 m, and depth 0.6 m) located at the Hydraulics Laboratory of the University of Palermo (Carollo and Ferro, 2021). The large-scale disturbances due to inflow conditions were avoided by locating the measuring reach (length 3 m) at 7.9 m from the inflow section. In this reach, PVC hemispheres, having a height $d = 0.03$ m (diameter of 0.06 m), were glued to the flume bed using a staggered mesh arrangement characterized by the same transversal and longitudinal distance between two elements (Fig. 1c). Three different concentrations of hemispheres C_h (Fig. 2) of 9, 25, and 49% were tested. A single value of slope s, equal to 0.5%, was tested. A concentric orifice plate was installed in the feed pipe to measure water discharge. Piezometers, connected with the flume bed, were used to measure water depth between roughness elements using the flume bottom as reference level. The water depth h was assumed equal to the average flow depth obtained by three piezometers. According to Lawrence (2000), this definition was preferred as it is simply based on measured data and does not need the estimate of variables related to roughness geometry. For the examined staggered arrangement, the aspect ratio B/h of the experimental runs varies between 2.5 and 59.7. These values demonstrate that no significant 3D effects and velocity dip phenomena occur for the

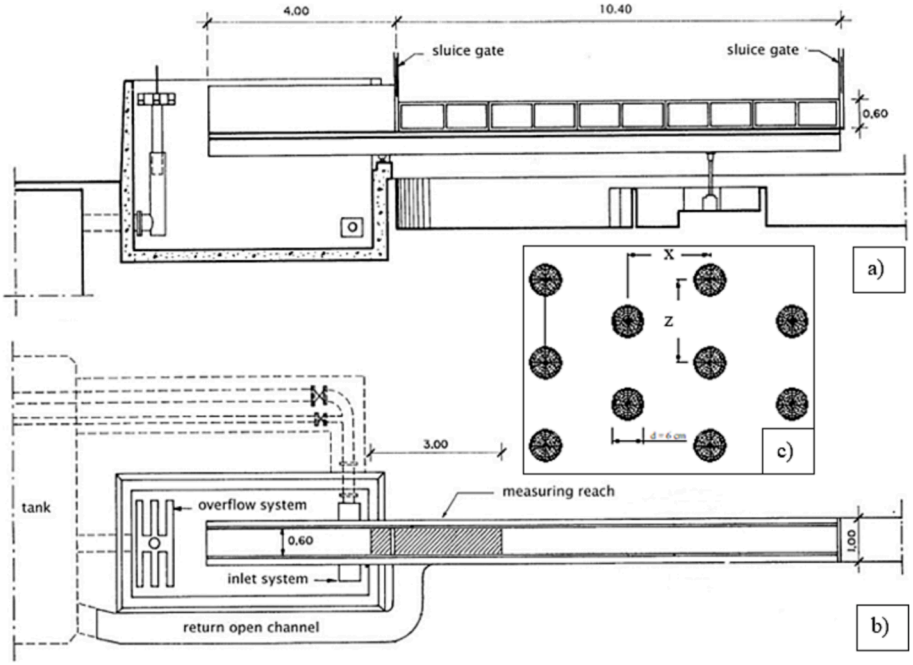

Fig. 1. Longitudinal (a) and plan (b) schemes of the experimental flume used to carry out the measurements and scheme of the experimental reach with a staggered arrangement of the hemispheres (c).

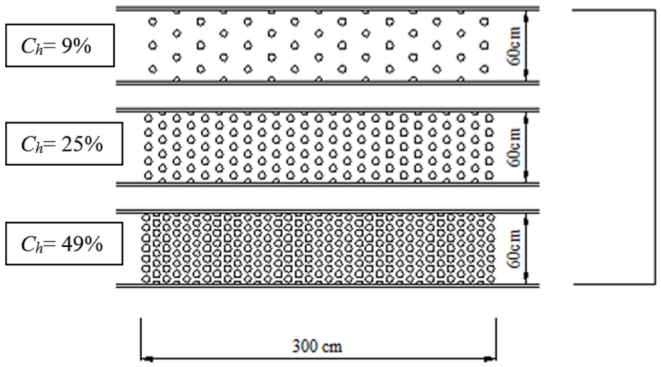

Fig. 2. Sketch of the three investigated boulder concentration *Ch*.

majority of the investigated experimental runs (43 of 55 are characterized by $B/h \geq 4$). The mean flow velocity V was calculated by the measured values of discharge Q and water depth h. According to Lawrence (1997), Lawrence (2000), the 55 experimental measurements were carried out for three different hydraulic conditions (partially submerged flow regime, $h/d < 1$ (16.4% of cases); marginally submerged flow regime, $1 \leq h/d \leq 2$ (25.4% of cases); completely-submerged flow regime, $h/d > 2$ (58.2% of cases) (Fig. 3). Table 1 reports for each investigated C_h the ranges of flow Reynolds number Re, Froude number F, and submergence ratio h/d, distinguishing between the partially submerged (9 data) and the submerged (46 data) conditions.

3. Results

As abovementioned, Lawrence (1997) suggested that the flow resistance on rough granular surfaces should be modelled using the submergence ratio. For the partially inundated flow regime ($h/d < 1$), the flow resistance is due to the drag effect of each roughness element, and it increases with the flow depth and element concentration. For $1 \leq h/d \leq 2$, the size of the elements affects the flow-vertical mixing, and frictional resistance tends to decrease very rapidly for increasing flow depths. For the well-submerged flow regime ($h/d > 2$), the flow is characterized by a more gradual decrease of f with increasing h, as compared to that observed during marginal submergence. Fig. 3 shows that the measurements (f, h/d), characterized by different concentrations, belong to the three flow regimes suggested by Lawrence (1997). In

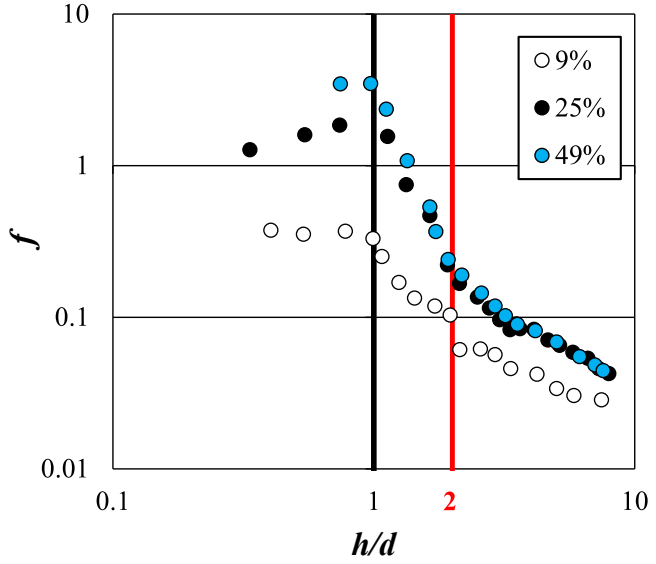

Fig. 3. Relationship between the friction factor f values and the h/d ratio for the investigated concentrations.

Table 1
Characteristic data of the experimental runs.

Condition	C_h %	h/d	Re	F
$h/d < 1$	9	0.40–0.99	1073–4061	0.32–0.33
	25	0.33–0.74	445–1145	0.14–0.17
	49	0.74–0.97	842–1218	0.10–0.10
$h/d \geq 1$	9	1.07–7.45	5183–142105	0.38–0.91
	25	1.13–7.94	2231–122883	0.15–0.73
	49	1.12–7.56	1783–115306	0.12–0.71

particular, the value $h/d = 1$ is a threshold between a increasing trend of f for $h/d < 1$, even if this trend is detected with a restricted number of measured pairs (h/d, f), and a decreasing trend of the friction factor with the submergence ratio for $h/d > 1$. For the investigated boulder concentrations, Fig. 3 also highlights that, for $h/d < 1$, f always increases with the element concentration. The higher energy dissipation, caused by the total drag resistance of the roughness elements, is explainable with the higher number of hemispheres and, consequently, the concentration. For this submergence regime and a fixed concentration value, f tends to increase, especially for $C_h = 25\%$, with h due to the increase of the drag resistance of each roughness element. For $h/d \geq 2$ and $C_h \leq 25\%$, f increases with C_h, whereas it does not vary anymore with the element concentration for $C_h > 25\%$. This finding can be physically explained by the fact that for higher values of C_h the elements are close and the formation of confined eddies between them occurs.

At first, since a single s value was used, the 55 measurements carried out for the staggered arrangement were used to calibrate Eq. (8), obtaining the following result:

$$\Gamma_v = 7.387F^{1.1154} \tag{9}$$

characterized by a coefficient of determination of 0.996. Fig. 4a shows the comparison between the Γ_v values obtained by Eq. (5), with α calculated by Eq. (6), and those calculated by Eq. (9).

Considering that Re^{δ} is always equal to 4.4817, and coupling Eq. (9) with Eq. (3) and Eq. (4), the following equation to estimate the Darcy–Weisbach friction factor is obtained:

$$f = 8\left[\frac{2^{1-\delta}4.4817}{(\delta+1)(\delta+2)}\right]^{-\frac{2}{1+\delta}}\left[\frac{1}{7.387F^{1.1154}}\right]^{2/(1+\delta)} \tag{10}$$

Fig. 4b shows the comparison between the measured f values and those calculated by Eq. (10) and demonstrates that an accurate estimate of the Darcy-Weisbach friction factor can be obtained by the proposed approach which uses the estimates of Γ obtained by Eq. (9) calibrated using the available 55 measurements. The friction factor values calculated by Eq. (10) are characterized by errors in estimate $E = (f_c - f_m)/f_m$ which are always less than or equal to ±20% and less than or equal to ±10% for 85.4% of cases.

Secondly, the database was used to test the Γ_v equation obtained by the measurements conducted for a square arrangement (Fig. 5a) by Carollo and Ferro (2021), Eq. (7) with $a = 0.3317$, $b = 1.1011$, and $c = 0.5795$. This choice is due to the fact that these Authors carried out their experiment using the same flume and hemispheres. Consequently, the comparison between the results allows determining the differences exclusively due to the different arrangements on flow resistance law. Fig. 5b shows the comparison between the measured f values and those calculated by the theoretical flow resistance law with Γ_v calculated with the latest values of a, b, and c estimated for the square arrangement. In this case, the friction factor values are characterized by errors in estimate $E = (f_c - f_m)/f_m$ which are less than or equal to ±20% for 96.4% of cases and less than or equal to ±10% for 78.2% of cases.

Fig. 6, which plots the pairs (f, h/d), shows that the Darcy-Weisbach friction factor values are different for the two arrangements (Fig. 6a for

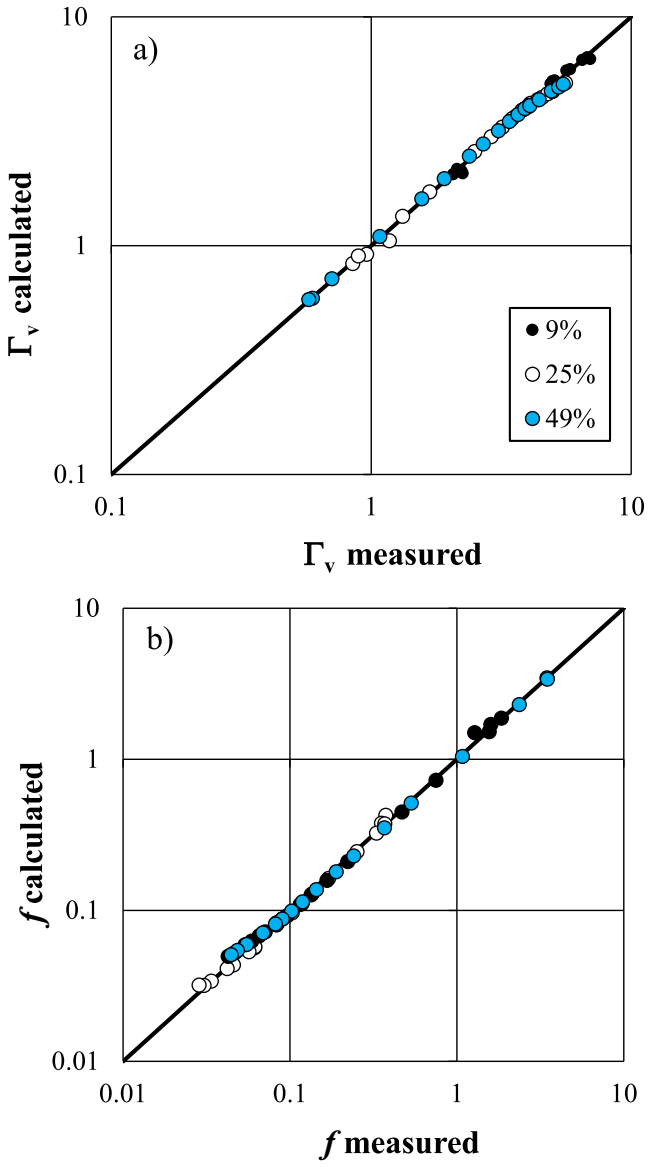

Fig. 4. Comparison between the Γ_v values obtained by Eq. (6), with $\alpha = 0.122$, and those calculated by Eq. (10) (a), and between the measured f values and those calculated by Eq. (11) (b).

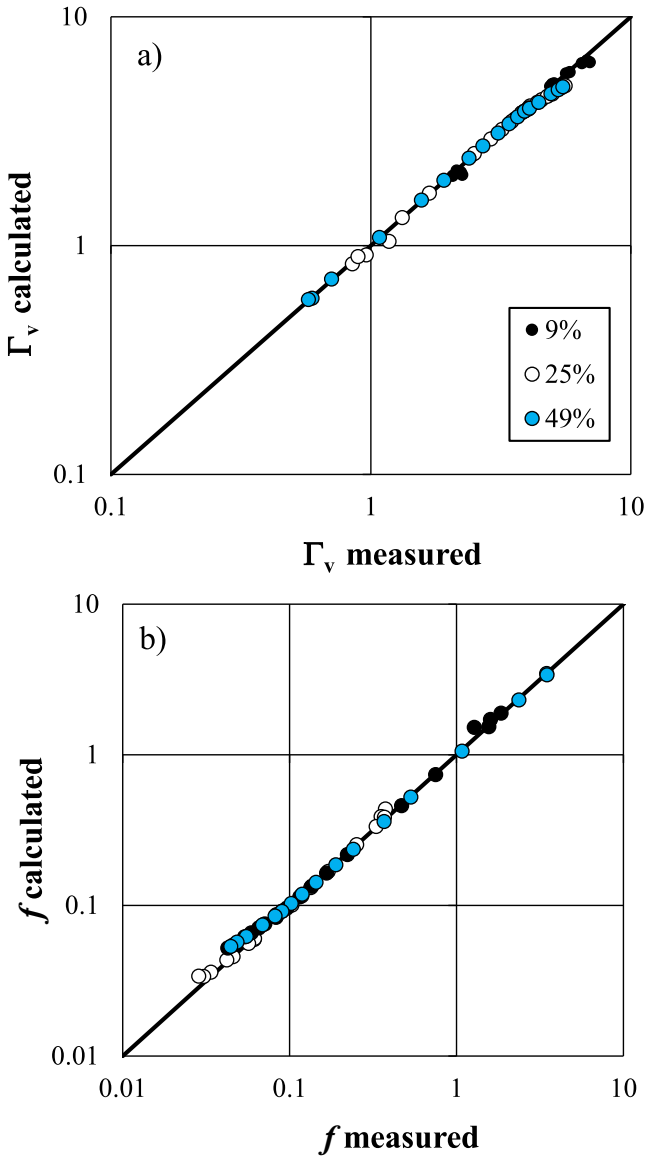

Fig. 5. Comparison between the Γ_v values obtained by Eq. (6), with $\alpha = 0.122$, and those calculated by Eq. (8) with $a = 0.3317$, $b = 1.1011$, and $c = 0.5795$ (a), and between the measured f values and those calculated by the theoretical flow resistance law with Γ_v calculated by Eq. (8) with $a = 0.3317$, $b = 1.1011$, and $c = 0.5795$ (b).

$C_h = 9\%$ and Fig. 6b for $C_h = 25\%$) up to the threshold of $h/d = 1$, while for $h/d > 1$ the curves tend to overlap.

Fig. 7, which plots the pairs (f, Re), shows that the Darcy-Weisbach friction factor values are different for the two arrangements (Fig. 7a for $C_h = 9\%$ and Fig. 7b for $C_h = 25$) up to a certain value of Reynolds number. From these values of Re, the curves of the two examined arrangements are overlapped.

4. Discussion

Notwithstanding the few pairs (h/d, f) corresponding to the condition $h/d < 1$ (partially submerged flow regime), Fig. 3 shows that flow resistance tends to increase with the submergence ratio, especially for $C_h = 25\%$. This result is due to the circumstance that, for a partially submerged flow regime, the increase of water depth determines an increase of the hemisphere cross-section hit by the flow and a consequent increase of flow resistance due to drag effects. For $1 < h/d < 2$ (marginally submerged flow regime), a rapid decrease of the flow resistance occurs when the submergence ratio increases. This rapid decrease is caused by the fact that, from the condition of $h/d = 1$, if the flow discharge increases, the water depth negligibly increases. This phenomenon is due to the formation of stable eddies confined between an element and the following one. Finally, for $h/d > 2$ (completely-submerged flow regime), flow resistance decreases for increasing h/d, but less rapidly than marginally submerged flow regime. This result agrees with the findings by Lawrence (1997) and Carollo and Ferro (2021).

Also, the element concentration affects the flow resistance determining increasing f values with C_h, with more significant differences for the partially inundated flow regime. In particular, Fig. 3 also highlights that, for $h/d < 1$, the flow resistance increases with C_h, while, for $h/d > 1$, the curves are overlapped for $C_h = 25$ and 49%. This result means that for partially inundated flow regime the element concentration affects flow resistance, while for inundated flow regime a skimming flow occurs for concentrations higher than 25%. Lawrence (2000) noticed that (a) when the roughness is fully submerged, flow resistance drops off very rapidly and this trend continues for increasing flow depth values and (b)

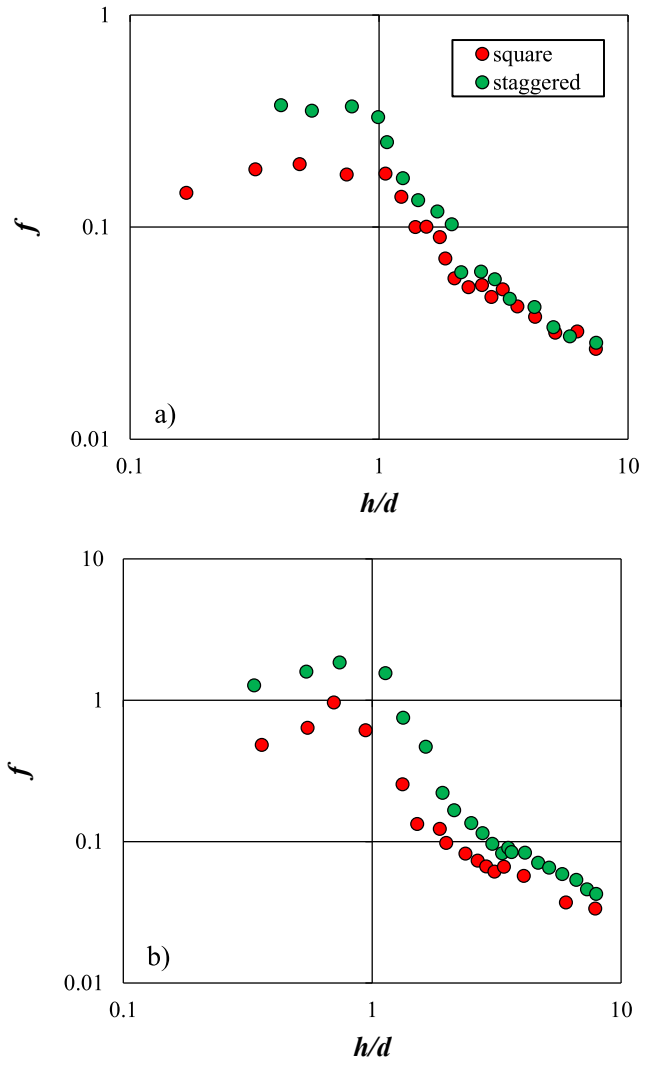

Fig. 6. Pairs (f, h/d) for staggered and square arrangements for $C_h = 9\%$ (a) and $C_h = 25\%$ (b).

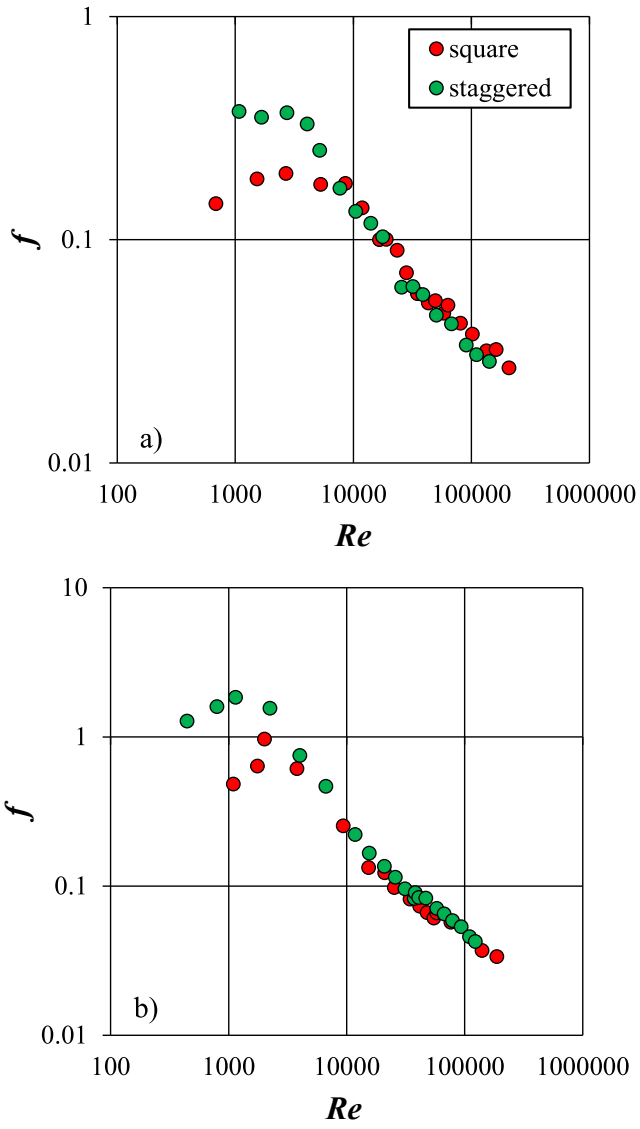

Fig. 7. Pairs (f, Re) for staggered and square arrangements for $C_h = 9\%$ (a) and $C_h = 25\%$ (b).

when the roughness is partially submerged ($h/d < 1$) the increase of the element concentration contributes to higher flow resistance.

Carollo and Ferro (2021) found that, for a square arrangement, the skimming flow occurs for element concentrations $\geq$50%. Consequently, for the staggered arrangement the skimming flow is reached for lower element concentrations as compared to the square one. This result is due to the fact that, for the same element concentration, the formation of skimming flow is influenced by the presence of the central element of the staggered arrangement. Whereas, for the square arrangement a smaller value of distance between two consecutive elements (i.e., a higher element concentration) is required for the occurrence of the skimming flow due to the absence of the central element.

Fig. 4 highlights that the presented theoretical approach guarantees a good estimate of the Darcy-Weisbach friction factor. In particular, the calibration of Eq. (9), using the measurements obtained for the staggered arrangement, gave the best results in terms of errors estimating f. Nevertheless, applying Eq. (7) with $a = 0.3317$, $b = 1.1011$, and $c = 0.5795$, calibrated by experimental data obtained for a square arrangement, led to a slight decrease in the accuracy in the estimate of the Darcy-Weisbach friction factor (Fig. 5). This result is probably due to the fact that the more significant differences in flow behavior occur for the partially submerged flow regime, and the measurements available for both arrangements for this flow regime were few, determining no differences between the two examined arrangements. In fact, for low values of water depth ($h/d < 1$ i.e., partially submerged flow regime), the staggered arrangement is characterized by a wider element cross-section hit by the flow as compared to the square one which determines a higher flow resistance (Fig. 6). In other words, a square array has a lower flow-facing obstacle area than a staggered one with the same element concentration, and therefore exerts less drag and a lower flow resistance.

Instead, for $h/d > 1$ the differences in terms of flow resistance between the two arrangements tend to reduce because the effect of the arrangement becomes more and more negligible (Fig. 6).

Finally, Fig. 7 shows that for $Re > 7700$–8500 for $C_h = 9\%$ (Fig. 7a) and $Re > 3779$–4000 for $C_h = 25\%$ (Fig. 7b) the differences in flow resistance between the two arrangements flatten. This last result is due to the circumstance that all these measurements are carried out for a turbulent flow regime. On the contrary, the most important differences in flow resistance occur for a laminar flow regime. This result can be justified considering that a flow characterized by a laminar flow regime is influenced by the additional drag resistance due to the increase of the hemisphere cross-section, while a flow characterized by a turbulent flow regime is not affected by the different element arrangement.

5. Conclusions

Gravel bed flow resistance is affected by the shape and size of the roughness elements and their arrangement on the channel bed surface (spacing between elements, direction with respect to flow streamlines, and protrusion of the elements from the channel bed).

Many investigations available in the literature demonstrated that the flow resistance of an open channel flows can be obtained integrating the power velocity profile. The main objective of this paper is to investigate these effects in gravel-bed channels characterized by different boulder concentrations using experiments performed with a staggered arrangement of the elements. At first, the measurements of flow velocity, and water depth obtained by a laboratory flume, covered by hemispheric elements with a staggered arrangement for two different hydraulic conditions (partially submerged and submerged) and three different concentrations, were used to calibrate the Γ function of the power velocity profile. For studying the effect of the element arrangement on flow resistance, the flow resistance law, obtained by literature measurements carried out with the same experimental setup but with a square arrangement, was tested for the measurements obtained with the staggered arrangement. The results highlighted that i) the flow resistance law gives a good estimate of the Darcy-Weisbach friction factor, ii) the differences in flow resistance behavior between the two different investigated arrangements mainly occur for the partially inundated condition due to the additional drag resistance due to the increase of the hemisphere cross-section, and iii) for the staggered arrangement the skimming flow is reached for lower element concentrations as compared to the square one.

Declaration of Competing Interest

The authors declare that they have no known competing financial interests or personal relationships that could have appeared to influence the work reported in this paper.

Data availability

Data will be made available on request.

Acknowledgements

All the Authors developed the theoretical analysis, analyzed the results and contributed to writing the paper. This research did not receive any specific grant from funding agencies in the public, commercial, or not-for-profit sectors.

References

Baiamonte, G., Ferro, V., Giordano, G., 1995. Advances on velocity profile and flow resistance law in gravel bed rivers. Excerpta 9, 41–89.
Barenblatt, G.I., 1987. Dimensional Analysis. Gordon & Breach, Science Publishers Inc., Amsterdam.
Barenblatt, G.I., 1991. On the scaling laws (incomplete self-similarity with respect to Reynolds numbers) for the developed turbulent flows in tubes. C.R Acad. Sci. Ser. II 13, 307–312.
Barenblatt, G.I., 1993. Scaling laws for fully developed turbulent shear flows, part 1, Basic hypothesis and analysis. J. Fluid Mech. 248, 513–520.
Bathurst, J.C., 1978. Flow resistance of large-scale roughness. J. Hydraulic Eng. ASCE 104 (12), 1587–1603.
Bathurst, J.C., 1982. Flow resistance in boulder-bed streams. In: Hey, R.D., Bathurst, J.C., Thorne, C.R. (Eds.), Gravel-bed Rivers. Wiley, Chichester, pp. 443–462.
Bathurst, J.C., 1985. Flow resistance estimation in mountain rivers. Proc. ASCE. J. Hydraulic Eng. 111 (4), 625–643.
Bathurst, J.C., Li, R.H., Simons, D.B., 1981. Resistance equations for largescale roughness. J. Hydraulic Eng. ASCE 107, 1593–1613.
Bathurst, J.C., 1988. Velocity profile in high-gradient, boulder-bed channels. In: Proceedings of International Conference on Fluvial Hydraulics, IAHR, Budapest. 29-34.
Bray, D.I., 1979. Estimating average velocity in gravel bed rivers. Proc. ASCE. J. Hydraulic Eng. 105 (9), 1103–1122.
Bray, D.I., 1982. Flow resistance in gravel-bed rivers. In: Hey, R.D., Bathurst, J.C., Thorne, C.R. (Eds.), Gravel-Bed Rivers. Wiley, Toronto, pp. 109–132.
Bray, D.I., 1987. A review of flow resistance in gravel bed rivers. In: Proc. of the Workshop "Leggi morfologiche e loro verifiche di campo", pp. 23-57 (Ed. Bios, Cosenza, Italy).
Carollo, F.G., Ferro, V., 2021. Experimental study of boulder concentration effect on flow resistance in gravel bed channels. Catena 205, 105458. https://doi.org/10.1016/j.catena. 2021.105458.
Castaing, B., Gagne, Y., Hopfinger, E.J., 1990. Velocity probability density functions of high Reynolds number turbulence. Physica D 46 (2), 177–200.
Chen, X., Hassan, M.A., An, C., Fu, X., 2020. Rough correlations: meta-analysis of roughness measures in gravel bed rivers. e2020WR027079 Water Resour. Res. 56 https://doi.org/10.1029/2020WR027079.
Coleman, N.L., Alonso, C.V., 1983. Two-dimensional channel flows over rough surfaces. J. Hydraulic Eng. ASCE 109 (2), 175–188.
Colosimo, C., Copertino, V.A., Veltri, M., 1988. Friction factor evaluation on gravel bed rivers. J. Hydraulic Eng. ASCE 114, 861–869.
Ferguson, R., 2007. Flow resistance equations for gravel and boulder bed streams. Water Resour. Res. 43, W05427. https://doi.org/10.1029/2006WR005422.
Ferro, V., 1999. Friction factor for gravel-bed channel with high boulder concentration. J. Hydraulic Eng. ASCE 125 (7), 771–778.
Ferro, V., 2003a. ADV measurements of velocity distributions in a gravel-bed flume. Earth Surf. Proc. Land. 28, 707–722. https://doi.org/10.1002/esp.467.
Ferro, V., 2003b. Flow resistance in gravel-bed channels with large-scale roughness. Earth Surf. Proc. Land. 28, 1325–1339. https://doi.org/10.1002/esp.589.
Ferro, V., 2017. New flow resistance law for steep mountain streams based on velocity profile. J. Irrigat. Drainage Eng., ASCE 143 (04017024), 1–6. https://doi.org/10.1061/(ASCE)IR.1943-4774.0001208.
Ferro, V., 2018. Assessing flow resistance in gravel bed channels by dimensional analysis and self-similarity. Catena 169, 119–127.
Ferro, V., Baiamonte, G., 1994. Flow velocity profiles in gravel bed rivers. J. Hydraulic Eng. ASCE 120 (1), 60–80.
Ferro, V., Giordano, G., 1991. Experimental study of flow resistance in gravel bed rivers. J. Hydraulic Eng. ASCE 117 (10), 1239–1246.
Ferro, V., Pecoraro, R., 2000. Incomplete self-similarity and flow velocity in gravel bed channels. Water Resour. Res. 36 (9), 2761–2769.
Ferro, V., Porto, P., 2018a. Applying hypothesis of self-similarity for flow resistance law in Calabrian gravel-bed rivers. J. Hydraulic Eng., ASCE 144 (04017061), 1–11.
Ferro, V., Porto, P., 2018b. Assessing theoretical flow velocity profile and resistance in gravel bed rivers by field measurements. J. Agric. Eng. Volume XLIX 810, 220–227.
Ferro, V., Porto, P., 2019. Closure to "Applying Hypothesis of Self-Similarity for Flow-Resistance Law in Calabrian Gravel-Bed Rivers" by Vito Ferro and Paolo Porto. J. Hydraulic Eng., ASCE 145(4), 07019002, 1–3.
Griffiths, G.A., 1981. Flow resistance in coarse gravel-bed rivers. Proc. ASCE. J. Hydraulic Div. 107 (7), 899–918.
Kellerhals, R., 1967. Stable channels with gravel-paved bed. Proc. ASCE. J. Waterways Harbour Div. 93, 63–84.
Kirkgöz, M.S., 1989. Turbulent velocity profiles for smooth and rough open channel flow. J. Hydraulic Eng. ASCE 115 (11), 1543–1561.
Lawrence, D.S.L., 1997. Macroscale surface roughness and frictional resistance in overland flow. Earth Surf. Proc. Land. 22 (4), 365–382.
Lawrence, D.S.L., 2000. Hydraulic resistance in overland flow during partial and marginal surface inundation: experimental observation and modelling. Water Resour. Res. 36 (8), 2381–2393.
Marchand, J.P., Jarrett, R.D., Jones, L.L., 1984. Velocity profile, water surface slope, and bed material size for selected streams in Colorado. US Geological Survey, Open-File Report 84–773.
Mendicino, G., Colosimo, F., 2019. Analysis of flow resistance equations in gravel-bed rivers with intermittent regimes: Calabrian fiumare Data Set. Water Resour. Res. 55, 7294–7319. https://doi.org/10.1029/2019WR024819.
Morris, H.M., 1959. Design methods for flow in rough conduits. Proc. ASCE J. Hydraulic Eng. 85 (7), 43–62.
Nicosia, A., Carollo, F.G., Ferro, V., 2023. Effects of boulder arrangement on flow resistance due to macro-scale bed roughness. Water 15, 349. https://doi.org/10.3390/w15020349.
Nitsche, M., Rickenmann, D., Kirchner, J.W., Turowski, J.M., Badoux, A., 2012. Macroroughness and variations in reach-averaged flow resistance in steep mountain streams. Water Resour. Res. 48, W12518. https://doi.org/10.1029/2012WR012091.
O'Loughlin, E.M., Macdonald, E.G., 1964. Some roughness-concentration effects on boundary resistance. La Houille Blanche 50 (7), 773–783.
Powell, D.M., 2014. Flow resistance in gravel-bed rivers: Progress in research. Earth Sci. Rev. 136, 301–338.
Pyle, R., Novak, P., 1981. Coefficient of friction in conduits with large roughness. J. Hydraul. Res. 19 (2), 119–140.
Reid, D.E., Hickin, E.J., 2008. Flow resistance in steep mountain streams. Earth Surf. Proc. Land. 33, 2211–2240. https://doi.org/10.1002/esp.1682.
Rickenmann, D., Recking, A., 2011. Evaluation of flow resistance in gravel-bed rivers through a large field data set. Water Resour. Res. 47, W07538. https://doi.org/10.1029/2010WR009793.
Rouse, H., Ince, S., 1963. History of Hydraulics. Dover Publications, New York.
Singh, P.K., Khatua, K.K., Banerjee, S., 2021. Flow resistance in straight gravel bed in bank flow with analytical solution for velocity and boundary shear distribution. ISH J. Hydraul. Eng. 27 (1), 9–22. https://doi.org/10.1080/09715010.2018.1505561.
Smart, G.M., Duncan, M.J., Walsh, J.M., 2002. Relatively rough flow resistance equations. J. Hydraul. Eng. 128 (6), 568–578.

Thompson, S.M., Campbell, P.L., 1979. Hydraulics of a large channel paved with boulders. J. Hydraul. Res. 17 (4), 341–354.
Yen, B.C., 2002. Open channel flow resistance. Proc. ASCE J. Hydraul. Eng. 128 (1), 20–39.
Zexing, X., Chenling, Z., Qiang, Y., Xiekang, W., Xufeng, Y., 2020. Hydrodynamics and bed morphological characteristics around a boulder in a gravel stream. Water Supply 20 (2), 395–407.